CHAPTER 2

NANOSCALED TRANSITION METAL OXIDES: A REVIEW

2.1 Introduction of metal oxides

According to IUPAC definition, "transition metals are defined as those elements which have partially filled *d* orbital. The *d*-block elements in groups 3–11 are transition elements shown in Figure 2.1 [1]. The *f*-block elements, also called *inner transition metals* (the lanthanides and actinides), also meet this criterion because *d* orbital is partially occupied before the *f* orbital [2]". A number of transition metals have been used in various daily activities. Titanium has been employed in manufacturing cosmetics, jewelry, bicycle frames, hip joint replacement, paints and aircrafts etc. Iron has numerous applications in daily life from kitchen utensils, rings in spiral notebook to automobiles, ships, buildings, and in hemoglobin of human blood. Chromium has applications as pigments, protective plating on cars and automobiles to prevent corrosion and to make stainless steel.

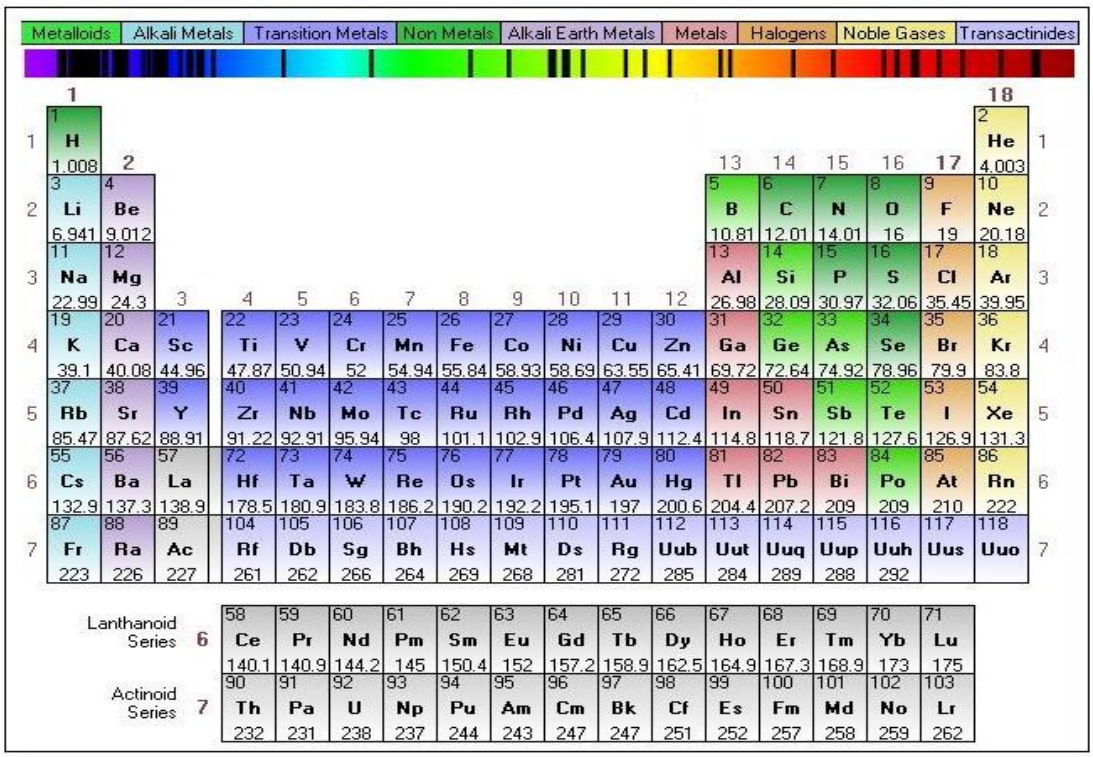

Figure 2.1: Periodic Table showing classifications of elements

Transition metals exhibit a broad range of chemical behavior. A few transition metals have high reduction potential which lead to their applications in making electronic

circuits and jewelry e. g. gold and platinum. On the other hand, lanthanides have strong tendency of oxidation. The transition metals can react with other elements in periodic table to form a number of compounds namely halides ($FeCl_2$, $CoBr_2$, NiF_2), oxides (TiO_2, ZrO_2, ZnO, FeO), hydroxides ($Co(OH)_2$), carbonates ($NiCO_3$)and other salts ($BaCrO_4$) etc.

Selection of transition metal oxides

Transition metal oxides comprise one of the most promising families of solids, featuring various geometries and characteristics. The metal oxygen connection can be highly covalent, nearly ionic or metallic in nature depending on the type of elements and their synthesis route. The transition metal oxides have shown breakthrough applications in a wide area due to their unusual properties.

1. The metal oxides may own unique and valuable structural, electronic and optical characteristics. They can possess more than one structural phase. For example, zirconium oxide could exist in cubic, monoclinic or tetragonal at different temperatures.
2. These oxides have been employed in numerous catalysis reactions e.g. removal of organic dyes, dehydrogenation, selective oxidation and reduction which are greatly useful for industrial applications [3].
3. Transition metals can construct composites with multiple oxidation states, which make them a suitable choice for different device fabrication.

2.2 Benchmarking properties of nanoscaled transition metal oxides

The nanoscaled transition metal oxides possess unique structural, optical, magnetic and electrical properties because of their nano size and large surface density. The electrons show dual wave-particle nature quantum mechanically. The properties of a solid depend on how the electrons interact with the neighbors in the lattice. As quoted by Y. Tokura [4], "According to the Bloch theorem, for instance, an electron placed in a periodic lattice behaves like an extended plane wave. However, when the number of free electrons in a solid becomes comparable to the number of the constituent atoms and the mutual electron-electron interaction becomes strong, electrons may lose their mobility". These neighboring interactions dramatically affect the electronic as well as optical properties of nanosized transition metal oxides. The

interplay of structure, electronic and magnetic properties is the cause of motivation to study the physics of metal oxides in nano-range.

Metal oxide nanoparticles own exceptional physical and chemical properties due to high density of surface sites. The reduction of particle size influences structural, electronic, optical and chemical properties of any material. The quantum confinement effects caused due to presence of discrete, atom-like electronic states. Also, decrease in particle size enhances the conductivity and chemical reactivity of metal oxides [5, 6]. The optical conductivity is one of the primary properties of metal oxides which can be measured in terms of reflectivity and absorption. Reflectivity changes drastically as scattering is strongly size-dependent. Due to quantum-size confinement, absorption of light becomes both discrete-like and size-dependent. Metal oxides can exhibit ionic or mixed conductivity (ionic/electronic), which could be altered due to nanosize. The density of free electrons/holes is proportional to band gap energy according to the Boltzmann statistics. The amount of charge carriers present in an oxide can be improved by disturbing its stoichiometry. Metal oxides have applications in absorption and catalytic processes due to their reduction/oxidation as well as acid/base properties. The main aspects necessary for their use as absorbents or catalysts are (i) the coordination environment of surface atoms, (ii) the redox properties, and (iii) the oxidation state at surface layers. Both redox and acid/base properties are interconnected and improved due to large surface area of nanosize.

Among a large number of transition metal oxides, zirconium oxide (ZrO_2) and titanium oxide (TiO_2) have been chosen to synthesize and achieve the stabilization of their desired phases employable in various technological applications. A brief detail of properties of zirconium oxide (ZrO_2) and titanium oxide (TiO_2) are discussed as following:

Zirconium oxide (ZrO_2)

Zirconium (IV) oxide (ZrO_2), also renowned as zirconia, is a ceramic material of enormous technological importance having unique mechanical and chemical properties namely high mechanical strength, transformation toughness, high chemical stability, excellent corrosion resistance, low thermal conductivity, porosity, thermally stabilized surface area and higher melting point [7-9]. Zirconia is p-type semiconductor with large band gap which owns plentiful oxygen vacancies on its surface. The high ion exchange capacity and redox behavior make it employable as

catalysts [10]. In addition, high values of thermal stability and ionic conductivity of zirconia fit it as an appropriate component for refractory purposes and in oxygen sensors.

Crystal structure of zirconia

The polymorphic zirconia exhibits three crystal geometries with identical chemistry namely cubic (c), tetragonal (t) and monoclinic (m) which are shown in figure 2.2.

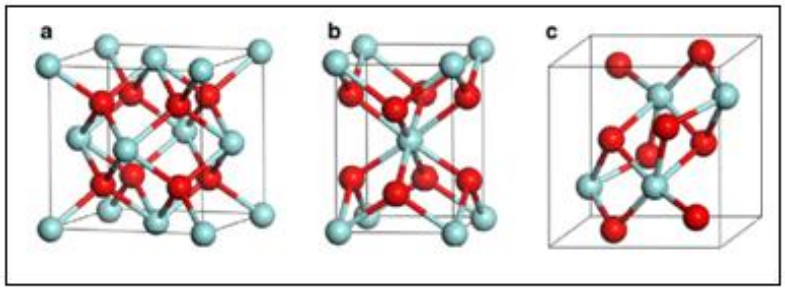

Figure 2.2: Crystalline geometries of zirconia (a) cubic (b) tetragonal (c) monoclinic (red and blue spheres represent oxygen and zirconium respectively). [11]

At room temperature, pure zirconia has monoclinic phase, which is stable up to 1170°C. The transformation of monoclinic to tetragonal occurs at temperature 1170°C and the tetragonal zirconia is found to be stable up to 2370°C.

$$(m)\text{-}ZrO_2 \underset{950^\circ C}{\overset{1170^\circ C}{\rightleftharpoons}} (t)\text{-}ZrO_2 \overset{2370^\circ C}{\rightleftharpoons} (c)\text{-}ZrO_2 \overset{2680^\circ C}{\rightleftharpoons} \text{liquid}$$

On further increasing the temperature, cubic phase of zirconia is formed. Interestingly, zirconia exhibits "**martensitic**" transformation on cooling [12] which is the key for transformation toughening. The martensitic transformation is athermal and diffusionless which ensures a high speed transformation. Furthermore, the t→m transformation is related to a considerable temperature hysteresis, volume expansion of about 4-5% and large shear strain (14-15%) [13]. This t→m phase transformation considerably improves strength and toughness of metastable zirconia [14]. This phenomenon of toughening is called transformation toughening, figure 2.3 show the scheme of the process. A remote macroscopic tensile stress arises as a crack initializes on surface of partially stabilized t-ZrO_2. This tensile stress causes t→m phase transformation at the tip of crack.

Table 2.1: Physical properties of zirconia (ZrO_2).

Physical properties	Value
Lattice parameters	
Cubic	a=5.07Å (ICDD # 00-007-0337)
Monoclinic	a=5.16Å,b=5.23Å,c=5.34Å,β=99.25° (ICDD#01-074-0815)
Tetragonal	a=b=3.59Å, c=5.18Å (ICDD # 01-079-1770)
Boiling point	4300°C
Color	White
Molecular weight	123.22 g/mol
Density	
Cubic	6.27 g/ml
Monoclinic	5.68 g/ml
Tetragonal	6.10 g/ml
Melting point	2900°C
Solubility	
Soluble in	Hydrofluoric acid, conc. Sulfuric acid, molten glass
Insoluble in	Water, alkalies, organic solvents
Entropy of formation	-46.5 cal
Heat of fusion at 25°C	20.8 kg cal./mol
Thermal conductivity	2.7 W/(m.K)

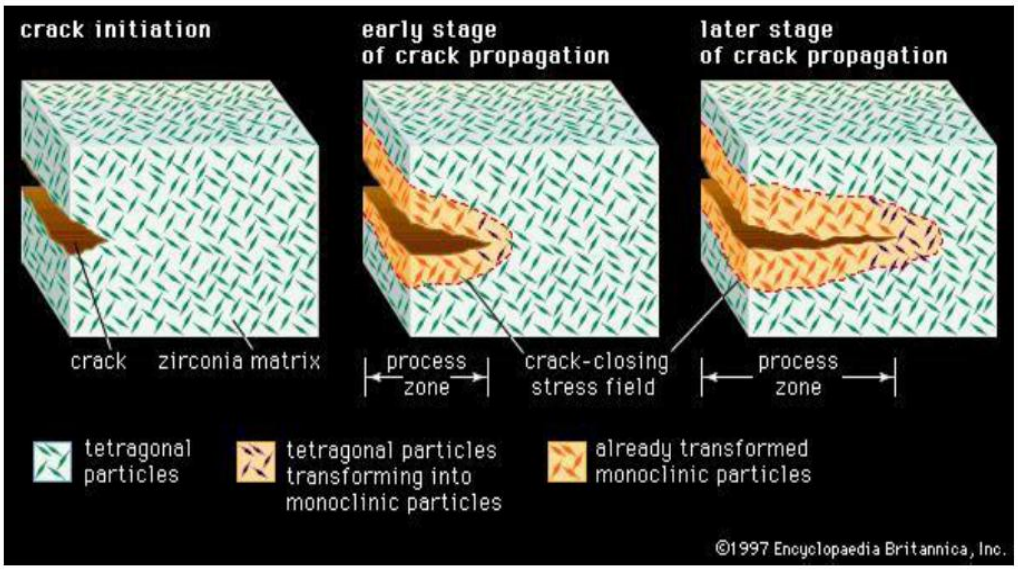

Figure 2.3: Scheme of transformation toughening process in zirconia

The physical properties of zirconia (ZrO_2) have been summarized in Table 2.1. The stabilization of zirconia is required for its applicability in device fabrication. Zirconia experiences disruptive phase changes on varying temperature. The phase changes can be eliminated by providing a support matrix or by adding small percentages of dopant, and the resulting material has superior thermal, mechanical, and electrical properties.

Titanium oxide (TiO_2)

Titanium dioxide, also renowned as titania, is a naturally occurring oxide of titanium with chemical formula TiO_2. Titania is well thought-out almost nearby to an ideal n-type semiconductor for photo-catalysis due to its high stability, low cost and non-toxic towards both humans and the environment. Titania is a white solid inorganic substance that is thermally stable, non-flammable, poorly soluble, and non-hazardous. It occurs naturally in several kinds of rocks and mineral sands. Titanium is the ninth most common element available in the earth's crust.

Crystal structure of titania

Titania particles naturally possess three crystalline forms: rutile, anatase, and brookite. Figure 2.4 shows ball and stick models of rutile, anatase and brookite [15, 16] where gray balls represent titanium atoms and red balls represents oxygen atoms. The most stable and abundant phase of titania is rutile which is chemically inert and can be excited in UV-visible range of electromagnetic spectra [15, 17]. On the other hand, anatase phase can only be excited by ultra-violet radiation and can be transformed into rutile on the increase of temperature. Both phases of zirconia exhibit a tetragonal di-pyramidal crystal system but possess individual space group lattices. Brookite hold orthorhombic crystal system and can be transformed into rutile on heating.

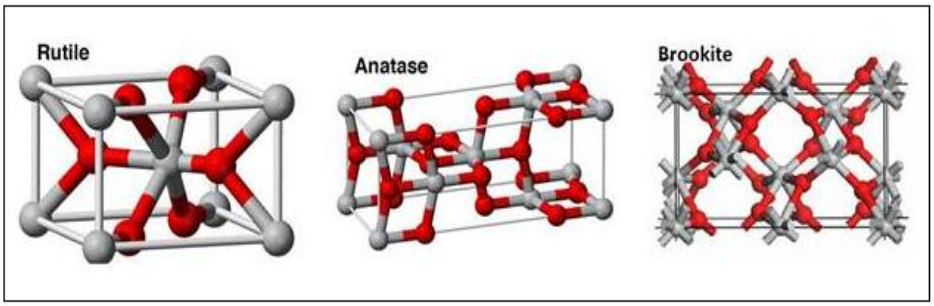

Figure 2.4: Balls-sticks models of rutile, anatase and brookite crystal forms of titania.

Titanium dioxide is a white, opaque, naturally occurring mineral and one of the most extensively applicable inorganic materials in device fabrication. It exists in a variety of crystal geometries; however, rutile and anatase are vital for technological applications. Both forms occur naturally; and can be mined and served as a source of commercial titanium. Titania is odorless, absorbent and soluble in concentrated acids. The surface area of titania particles is largest which makes it suitable photocatalysis and many others opto-electronic applications. Also, titania have high dielectric constant, good electrical conductivity as well as good thermal stability. Titanium dioxide is non-toxic and is chemically stable. The photocatalytic activity of titania thin coatings are acknowledged for its self-cleaning and disinfecting properties under exposure of ultraviolet radiation. The photocatalysis process exhibiting in titania is shown in Figure 2.5.

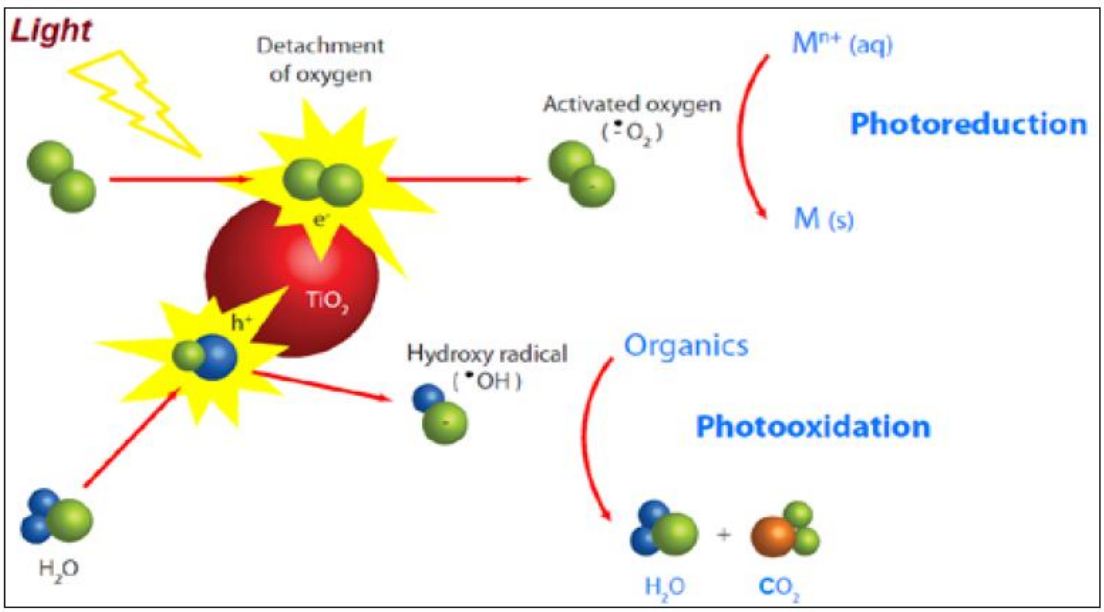

Figure 2.5: A general photocatalytic performance of Titania. [18]

The physical properties of titania has been tabulated in Table 2.2. All the three crystalline forms of titania have break through applications in various fields such as photovoltaic and photocatalytic devices, pigment, paints, coatings, sensors, solid oxide fuel cells etc. The stabilization of specific crystal form is desirable for device fabrication, which could be achieved by modifying synthesis route, growth conditions, thermal treatment and doping.

Table 2.2: Physical properties of titania (TiO_2)

Physical properties	Value
Lattice parameters	
Rutile	a=b=4.59Å, c=2.95Å (ICDD # 01-089-0555)
Anatase	a=b=3.73Å, c=9.37Å (ICDD # 00-001-0562)
Brookite	a=9.16Å, b=5.43Å, c=5.13Å (ICDD # 00-002-0514)
Boiling point	1843°C
Color	White
Molecular weight	79.86 g/mol
Density	
Rutile	4.06 g/ml
Anatase	3.90 g/ml
Brookite	4.14 g/ml
Melting point	2972°C
Solubility	
Soluble in	HF, conc. H_2SO_4
Insoluble in	Water, alkalies, organic solvents
Entropy of formation	50 $J/mol^{-1}K^{-1}$
Heat of fusion at 25°C	930 kJ/kg
Thermal conductivity	8.5 W/(m.K)

Silicon dioxide (SiO_2)

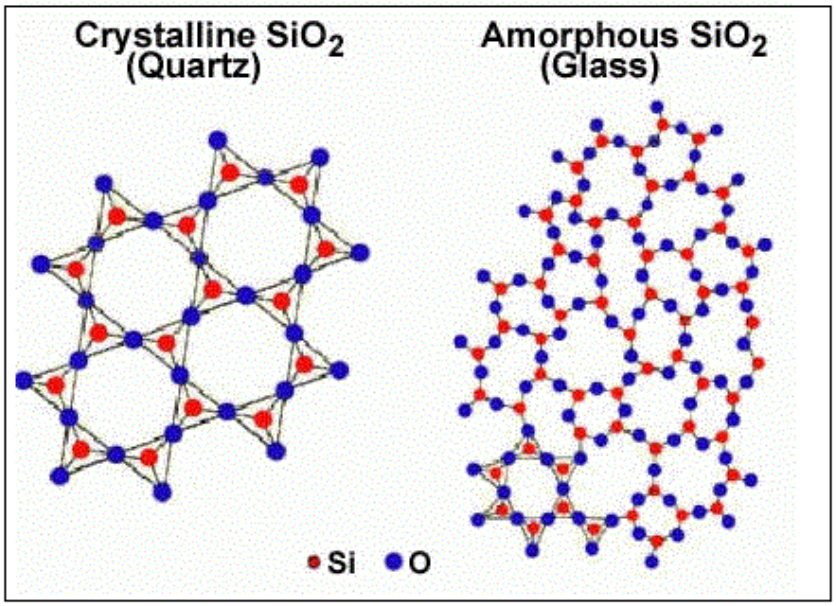

Figure 2.6: Crystal structure of quartz and amorphous silica.

Silicon dioxide, also renowned as silica is one of the most abundant mineral found in nature. Silica exhibits different crystalline geometries in addition to amorphous silica. The most talked crystalline form of silica is quartz which is the only stable form under normal conditions. The crystal structure of quartz and amorphous silica is shown in Figure 2.6 [19].

Crystalline quartz possesses hexagonal symmetry of crystal. Each silicon atom is tetrahedrally bonded to four oxygen atoms, and each oxygen atom (bridging atoms) is dihedrally bonded to two silicon atoms. It should be noted that each silicon atom shares its four oxygen atoms with another silicon atom, so the 1:2 stoichiometry is preserved and the silicon atom gets half of each of four oxygen atoms. In amorphous silica, some oxygen atoms will be bonded to only one silicon atom (non-bridging atoms). The local structure remains approximately the same, but the more macroscopic structure is randomized. The relative amount of bridging to non-bridging determines the "quality" of silica. The physical properties of silica have been listed in Table 2.3.

Table 2.3: Physical properties of silica (SiO_2).

Physical properties	**Value**
Lattice parameters	
Quartz (hexagonal)	a=b=4.90Å, c=5.39Å, γ=120° (ICDD # 00-001-0649)
Boiling point	2950°C
Color	white/colorless
Molecular weight	60.08 g/mol
Density	
Quartz	2.64 g/ml
Amorphous silica	2.19 g/ml
Melting point	1713°C
Entropy of formation	42 $J/mol^{-1}K^{-1}$
Heat of fusion at 25°C	930 kJ/kg
Thermal conductivity	
Quartz	12 W/(m.K)
Amorphous silica	1.4 W/(m.K)

Silica is the chief component in manufacturing of most glasses. The glass transition temperature of pure SiO_2 is ~1200°C. Molten silica when cooled quickly, does not crystallize but solidifies as a glass. The structural geometry of silicon and oxygen in glass is similar to that in quartz and most other crystalline forms of silica. The difference between the glass and crystalline forms arises from the connectivity of the tetrahedral units. Although there is no long range periodicity in the glassy network, ordering remains at length scales well beyond the Si-O bond length.

2.3 Prodigious applications of nanoscaled transition metal oxides

Metal oxide nanoparticles have numerous applications in various fields due to their unique and extraordinary properties. In general, metal oxide nanoparticles employed in sensors, photovoltaic devices, catalyst for photo-decomposition, pigments, cosmetics, semiconductors, refractory material, water and air treatment, electro-chromic devices, lasers, displays, photonics and anti-reflective coatings etc. The schematic diagram depicting various applications of metal oxide nanoparticles have been shown in Figure 2.7.

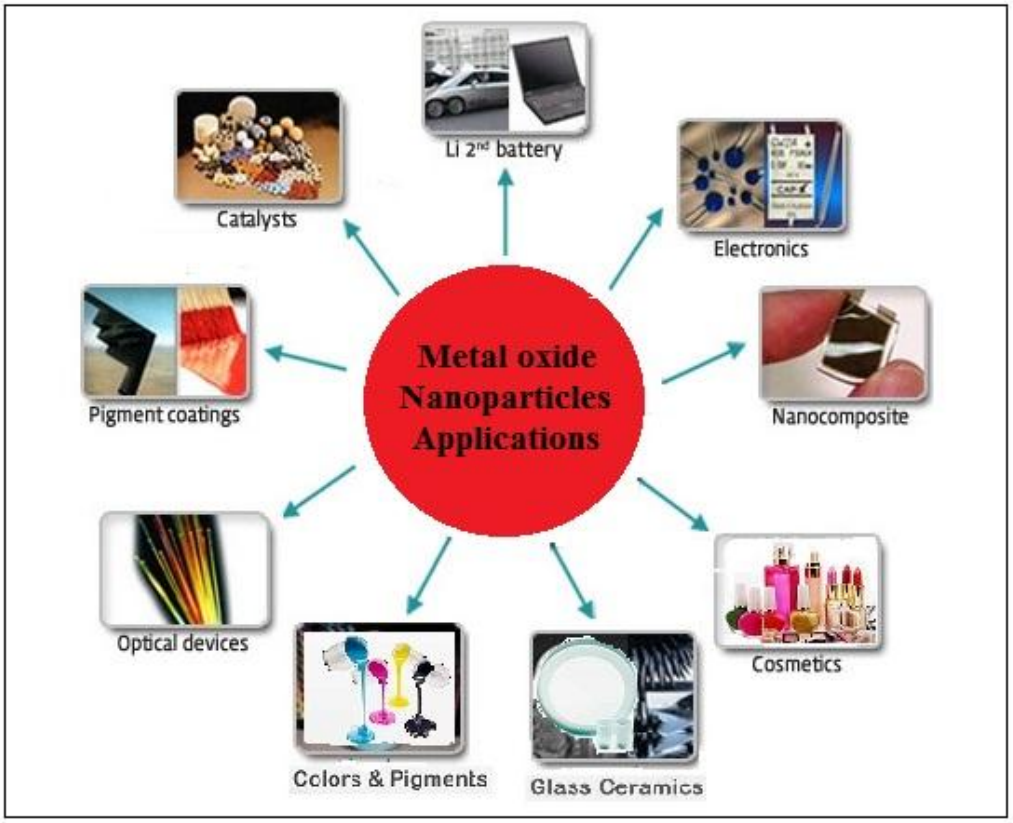

Figure 2.7: General applications of transition metal oxide nanoparticles.

A few applications of specific nanoparticles (NPs) are as follows:

1. Copper oxide NPs can be utilized as redox as well as oxidation catalyst. Also, CuO NPs can be used in photoconductive and photothermal processes.
2. Zinc oxide NPs can be used as UV blockers in sun locations, solar cells, gas sensors and as catalysts for organic reactions.
3. Zirconium oxide NPs can be employed in structural ceramics, solid electrolyte, gas sensors etc.
4. Magnesium oxide NPs are widely used as a scrubber for air pollutant gases (CO_2, NO_x, SO_x) as well as a catalyst in the organic synthesis.
5. Titanium oxide NPs are not only used in numerous catalytic processes but also in the materials science.
6. Cerium oxide NPs can be used as catalyst, luminescent and UV blocking material.

Zirconia (ZrO_2) has been extensively utilized in a number of technical devices [20], particularly in gas sensors, solid oxide fuel cells (SOFCs), catalysis, catalyst supports [21, 22] and orthopedic implants [23]. The high melting point of zirconia promotes it as a good refractory as well as thermally stable material. Due to low thermal conductivity, expansion coefficient and refractory characteristic, zirconia could be employed as thermal barrier coating in jet engines. Zirconia possesses high ionic conductivity mainly for oxygen ions which makes it suitable for high temperature fuel cells and oxygen sensors. Due to its good biocompatibility, high hardness and strength, zirconia frequently employed as orthopedic implants, such as femoral head component in hip implants and dental implants. In addition, zirconia is chemically and thermally stable combined with its unique amphoteric characteristic, makes it an ideal candidate for catalyst.

Titania (TiO_2) is acknowledged for its several versatile applications originating due to its unique crystal structure and semiconductor properties. These applications include UV absorbing transparent coatings, flip-flop automobile coatings, plastic additives, cosmetic UV blockers and electronic components characterized by rutile ultrafine particles. Anatase based applications are even more versatile and include photocatalysis (self-cleaning effect, decomposition of harmful nitrous oxides from

automobile exhausts, water and air purification), photo-electrochromic windows, dye-sensitized solar cells (DSSC) and many more. Also, titanate composites are utilized as photocatalysts for degradation of organic dyes used in textiles [24] and for photocatalytic hydrogen evolution [25].

2.4 Review of current research work

Due to the peculiar properties of nanosized materials, the research in the field of nanoscience and nanotechnology has become a thrust area of scientific interest globally and as a result many reviews have been published [26, 27]. There has been an increasing interest in research regarding the synthesis, properties and applications of metal oxides at international/national level. A. Kay and M. Grätzel [28] coated insulating large band gap oxides such as ZnO, TiO_2, ZrO_2, MgO, Al_2O_3, and Y_2O_3 on SnO_2 to enhance its photovoltaic performance. B. S. Richards [29] reported the deposition of TiO_2 thin films in amorphous, rutile and anatase phases using both ultra spray deposition (USD) and chemical vapour deposition (CVD) and studied their properties for photovoltaic applications. Yang et al. [30] loaded Nd doped titania to SiO_2 using sol-gel method and reported its photocatalytic activity with different neodymium contents. A. M. Gaur and co-workers [31] prepared the doped TiO_2 thin films on silicon wafers prepared by sol-gel spin coating technique and studied their structural, optical properties such as grain size and band gap.

A. Dhar et al. [32] prepared and studied properties of Er-doped ZrO_2 nanocrystalline phase separated preforms of optical fibers by MOCVD process. Zirconium oxide thin films loaded with 10, 30 and 50 mol% lanthanide ions (Er or Eu) have been successfully prepared photochemically, followed by a post annealing treatment process by G. Cabello et al. [33]. The resultant films were characterized by X-ray photoelectron spectroscopy, atomic force microscopy and photoluminescence. A samarium doped polycrystalline ZrO_2 bulk sample has been investigated for its phase composition as well as optical properties within the temperature range 6–300 K by S. Lange and co-workers [34]. A. Mikó and others [35] presented "A synthesis route for the preparation of mesoporous zirconia using spin-coating method combined with block copolymer templating evaporation induced self assembly (EISA) and characterized the films to study surface morphology". Ionic liquid-templated preparation of mesoporous silica embedded with nanocrystalline sulfated zirconia has been reported by A. J. Ward et al. [36]. "The physicochemical properties of prepared

materials were studied using characterization techniques such as inductively coupled optical emission spectroscopy, X-ray diffraction, transmission electron microscopy, energy-dispersive X-ray micro/elemental analysis, and X-ray photoelectron spectroscopy".

N. Agaudjil and co-workers [37] synthesized the mixed oxide ZrO_2-SiO_2 membranes by sol-gel technique to elaborate thin and porous layers with controllable porosity. Their results showed the great potentiality of inorganic membranes and allow new applications in waste water treatment and gas separation. Sol-gel zirconia has been prepared by X. Bokhimi et al. [38] with zirconium n-butaoxide and different hydrolysis catalysts such as HCl, H_2SO_4, $C_2H_4O_2$ and NH_4OH and characterized with various techniques. Microstructural and electrical conductivity properties of cubic zirconia doped with various amount of titania have been studied by S. Tekeli et al. [39]. Their results showed that when the TiO_2 amount was less than 5 wt%, the specimens were entirely single cubic phase; further addition of TiO_2 (5 wt% or more) caused the formation of tetragonal phase.

"Single-crystals of the rare earth pyrochlores were synthesized using a high-temperature flux technique and were subsequently characterized using single-crystal X-ray diffraction" by J. M. Farmer, L. A. Boatner and others [40]. The relation of lattice parameters with the RE-site cation radius was studied. Also, the coefficient of thermal expansion was estimated as $10.1–11.2 \times 10^{-6}$ °C^{-1}.

A series of pyrochlore $Ln_2Ti_2O_7$ (Ln = Sm, Gd, Dy, Er) nanocrystals were synthesized via stearic acid method (SAM) [41]. The structural and thermal characterizations of prepared pyrochlores were performed and the results were compared with traditional solid-state reaction (SSR). It was found that $Ln_2Ti_2O_7$ can be synthesized at relatively low temperature (700–800 °C) with shortened reaction time (2–4 h). The synthesis of thin films of thulium and ytterbium-doped titanium oxide, grown by metal-organic spray pyrolysis deposition, has been reported by S. Forissier et. al [42]. The anatase phase of TiO_2 was obtained and organic contamination was eliminated by annealing treatments. G. V. Khade, M. B. Suwarnkar and coworkers prepared "samarium doped TiO_2 nanoparticles by microwave assisted sol–gel method [43]. The photocatalytic activity of TiO_2 and Sm doped TiO_2 was investigated on the photocatalytic degradation of MO under UV and solar light irradiation". It was found that Sm doped TiO_2 shows about 10 % increment in the photocatalytic activity. G. N. Shao and his

co-workers [44] reported "a novel sol–gel method to synthesize pure TiO_2 and ZrO_2–TiO_2 samples by controlling the ratio of Zr-to-Ti between 0.75 and 3.2 to evaluate the effect of the amount of ZrO_2 in the composites. Abnormal grain growth (AGG) was unexpectedly observed in the samples calcined at higher temperatures ($\leq$ 800 °C). Comparisons of the activities of the samples towards decolorization of methylene blue indicated that the photocatalytic efficiencies of the composites with Zr/Ti $\leq$ 2.2 were superior to that of pure TiO_2".

Chemical spray pyrolysis (CSP) was used by A. Juma et. al. to dope TiO_2 thin films with Zr [45]. They found that "uniform and homogeneous Zr-doped TiO_2 thin films with much smaller grains than undoped TiO_2 films were formed. The optical band gap for TiO_2 decreased from 3.3 eV to 3.0 eV after annealing at 800°C but for the TiO_2:Zr(20) film it remained at 3.4 eV. The dielectric constant increased by more than four times with Zr-doping and this was associated with the change in the bond formations caused by substitution of Ti by Zr in the lattice". La-doped TiO_2 (La-TO) photocatalysts with visible-light-driven capacity for NO removal were successfully synthesized by Y. Huang et. al. via a facile sol-gel method [46]. The authors quoted that "3% La integrated with TiO_2 (in mass ratio) could enhance the removal efficiency of NO (up to 32%) under solar light, which is more than twice that seen with pure TiO_2". TiO_2 thin films, doped with Cerium, Dysprosium and Europium have been fabricated by spin-coating sol-gel method [47]. N. C. Bezir et. al. reported the presence of mixed rutile and the dominant anatase phases in Eu and Dy-doped samples, however Ce-doped samples consist of anatase phase only.

2.5 Summary

The chapter emphasizes the detailed introduction of nanoscaled metal oxides, their bench marking properties and prodigious applications. The definition of transition metal oxides and reason of their selection for research has been explained. The general properties of metal oxides along with characteristic properties of zirconia (ZrO_2), titania (TiO_2) and silica (SiO_2) have been discussed. And, moreover, the technological applications of metal oxides especially of zirconia (ZrO_2) and titania (TiO_2) has been mentioned in the above description. In the last, the current research work related to the problem of present thesis has been reviewed in brief.

References

1. IUPAC, *Compendium of Chemical Terminology*, 2nd ed. (1997). Online corrected version: "transition element", (2006).
2. H.H. Kung, Transition metal oxides: surface chemistry and catalysis, Elsevier, (1989).
3. Y. Tokura, Phys. Today **56** (2003) 50.
4. M. Fernandez-Garcia, J. C. Conesa, F. Illas, Surf. Sci. **349** (1996) 207.
5. J. A. Rodriguez, S. Chaturvedi, M. Kuhn, J. Hrbek, J. Phys. Chem. B **102** (1998) 5511.
6. A. Hirvonen, R. Nowak, Y. Yamamoto, T. Sekino, K. Niihara, J. Eur. Ceram Soc. **26** (2006) 1497.
7. J. C. Ray, D. W. Park,W. S. Ahn, Ind. Eng. Chem. Res. **12** (2006) 142.
8. R. Srinivasan, B. Davis, Proceed. Am. Chem. Soc. Symp.: Mat. Synth. Charact. (1997) 147.
9. J. L. Gole, S. M. Prokes, J. D. Stout, O. J. Glembocki, R. Yang, Adv. Mat. **18** (2006) 664.
10. Y. Han, J. Zhu, Top. Catal. **56** (2013) 1525.
11. P. Floratos, A. Goulas, Martensitic transformation analysis and transformation toughness on zirconia (ZrO_2) ceramics, Uni. of Thessaly, Volos, Greece.
12. T. Vagkopoulou, S. O. Koutayas, P. Koidis, J. R. Strub, Int. J. Esthet Den. **4** (2009) 130.
13. M. Bocanegra-Bernal, S. Dioz De La Torre, J. Mater. Sci. **37 (**2002) 4947.
14. R. Austin, S. F. Lim, PNAS **105** (2008) 17217.
15. S. Woodley, C. Catlow, Comput. Mater. Sci. **45** (2009) 84.
16. K. Hashimoto, H. Irie, A. Fujishima, Jpn. J. Appl. Phys. **44** (2005) 8269.
17. http://www.cinkarna.si/en/files/default/izdelki/tio2/uf_tio_as_highly_active_photocatalytic_material.pdf.
18. https://goo.gl/images/2QC59t.

19. A.O. Bianchi, M. Campanati, P. Maireles-Torres, E. R. Castellon, A. J. Lopez, A. Vaccari, Appl. Catal. A **220** (2001) 105.

20. R. Gomez, F. Tzompantzi, T. Lopez, O. Navaro, React. Kinet. Catal. Lett. **53** (1994) 245.

21. S. Damyanova, L. Petrov, M.A. Centeno, P. Grange, Appl. Catal., A **224** (2002) 271.

22. W. Wang, S. Liao, Y. Zhu, M. Liu, Q. Zhao, Y. Fu, J. Nanomat. (2015) Article ID 408643.

23. A. Nashim, K.M. Parida, Chem. Eng. J. **215-216** (2013) 608.

24. M. Uno, A. Kosuga, M. Okui, K. Horisaka, S. Yamanaka, J. Alloys Compd. **400** (2005) 270.

25. J. J. Mcclelland, Handbook of Nanostructured Materials and Nanotechnology, H. S. Nalwa (Ed.) Academic Press (2000) Ch. 7.

26. K. C. Kwaitkowski, C. M. Lukehart, Handbook of Nanostructured Materials and Nanotechnology, H. S. Nalwa (Ed.) Academic Press (2000) Ch. 8.

27. A. Kay, M. Gratzel, Chem. Mater. **14** (2002) 2930.

28. B. S. Richards, Ph. D Thesis, Uni. of New South Wales, Sydney, Australia (2002).

29. X. Yang, L. Zhu, L. Yang, W. Zhou, Y. Xu, Trans. Nonferrous Met. Soc. **21** (2011) 335.

30. A. M. Gaur, R. Joshi, M. Kumar, Proc. World Congress Eng., London (2011).

31. A. Dhar, I. Kasik, B. Dussardier, O. Podrazky, V. Matejec, Int. J. Appl. Ceram. Technol. 1-8, 2011.

32. G. Cabello, L. Lillo, C. Caro, G. E. Buono-Core, B. Chornik, M. A. Soto, J. Non-Cryst. Solids **354** (2008) 3919.

33. S. Lange, I. Sildos, M. Hartmanova, V. Kisik, E. E. Lomonova, M. Kirm, J. Phys.: Conf. Series **249** (2010) 012007.

34. A. Miko, A. L. Demirel, M. Somer, IOP Conf. Series: Mater. Sci. & Engg. **12** (2010) 012019.

35. A. J. Ward, A. A. Pujari, L. Costanzo, A. F. Masters, T. Maschmeyer, Nanoscale Res. Lett. **6** (2011) 192.

36. N. Agoujil, N. Benmouhoub, L. Labot, Desalination **184** (2005) 65.

37. X. Bokhimi, A. Morales, O. Novaro, M. Portilla, T. Lopez, F. Tzompantzi, R. Gómez, J. Solid State Chem. **135** (1998) 28.

38. S. Tekeli, A. Akcimen, O. Gurdal, M. Guru, J. Achiev. Mater. Manuf. Eng. **25** (2007) 39.

39. J. M. Farmer, L. A. Boatner, B. C. Chakoumakos, Mao-Hua Du, M. J. Lance, C. J. Rawn, J. C. Bryan, J. Alloys Compd. **605** (2014) 63.

40. W. Zhang, L. Zhang, H. Zhong, L. Lu, X. Yang, X. Wang, Mater. Charact. **61** (2010) 154.

41. S. Forissier, H. Roussel, P. Chaudouet, A. Pereira, J. Deschanvres, B. Moine, J. Therm. Spray Technol. **21** (2012) 1263.

42. G. V. Khade, M. B. Suwarnkar, N. L. Gavade, K. M. Garadkar, J. Mater. Sci.: Mater. Electronics **27**(2016) 642.

43. G. N. Shao, S.M. Imran, S. J. Jeon, M. Engole, N. Abbas, M. S. Haider, S. J. Kang, H. T. Kim, Powder Technol. **258** (2014) 99.

44. A. Juma, I. O. Acik, A.T. Oluwabi, A. Mere, V. Mikli, M. Danilson, M. Krunks, Appl. Surf. Sci. **387** (2016) 539.

45. Y. Huang, Jun-Ji Cao, F. Kang, Sheng-Jie You, Chia-Wei Chang, Ya-Fen Wang, Aerosol Air Qual. Res. **17** (2017) 2555.

46. N. C. Bezir , A. Evcin , R. Kayali , M. Ozen , G. Balyac, Acta Phys. Pol., A **132** (2017) 620.